[朝倉 正紀] Min K Asakura M (7 人略) Asanuma H (1 人略) Minamino T (5 人略) Furukawa H (1 人略) Takashima S (1 人略) Kitakaze M	Identification of genes related to heart failure using global gene expression profiling of human failing myocardium	Biochem. Biophys. Res. Commun.	393	55–60	2010
Sasaki H Asanuma H (5 人略) Asakura M (1 人略) Minamino T Takashima S (4 人略) Kitakaze M.	Metformin prevents progression of heart failure in dogs: role of AMP–activated protein kinase	Circulation	119	2568–2577	2009
Asakura M Kitakaze M	Global gene expression profiling in the failing myocardium.	Circ J	73	1568–1576	2009
Takahama H Minamino T Asanuma H (7 人略) Asakura M (1 人略) Takashima S (3 人略) Kitakaze M	M.Prolonged targeting of ischemic/reperfused myocardium by liposomal adenosine augments cardioprotection in rats	J Am Coll Cardiol	53	709–717	2009
Fujita M Asakura M (4 人略) Asanuma H (6 人略) Kitakaze M	Activation of ecto–5'–nucleotidase in the blood and hearts of patients with chronic heart failure	Journal of Cardiac Failure	14	426–430	2008
Liao Y Zhao H Ogai A Kato H Asakura M Kim J Asanuma H Minamino T Takashima S Kitakaze M	Atorvastatin slows the progression of cardiac remodeling in mice with pressure overload and inhibits epidermal growth factor receptor activation	Hypertens Res	31	335–344	2008

[筒井 裕之] Ohta Y (7人略) Tsutsui H	Oxidative stress impairs insulin signal in skeletal muscle and causes insulin resistance in post-infarct heart failure	Am J Physiol Heart Circ Physiol		In press	2010
Ikesue M (8人略) Tsutsui H Uede T	Syndecan-4 deficiency limits neointimal formation after vascular injury by regulating vascular smooth muscle cell proliferation and vascular progenitor cell mobilization	Arterioscler Thromb Vasc Biol		In press	2010
Hamaguchi S (8人略) Tsutsui H	Spironolactone use at discharge was associated with improved survival in hospitalized patients with systolic heart failure	Am Heart J	160(6)	1156-1162	2010
Tsutsui H Kinugawa S Matsushima S	Mitochondrial oxidative stress and dysfunction in myocardial remodelling	Cardiovasc Res	81	449-456	2009
Naya M Tsukamoto T (7人略) Tsutsui H	Myocardial beta-adrenergic receptor density assessed by 11C-CGP12177 PET predicts improvement of cardiac function after carvedilol treatment in patients with idiopathic dilated cardiomyopathy.	J Nucl Med	50(2)	220-225	2009
Suga T (9人略) Tsutsui H	Intramuscular metabolism during low-intensity resistance exercise with blood flow restriction.	J Appl Physiol	106	1119-1124	2009
Matsushima S (5人略) Tsutsui H	Increased myocardial NAD (P) H oxidase-derived superoxide causes the exacerbation of post-infarct heart failure in type 2 diabetes.	Am J Physiol Heart Circ Physiol	297	409-416	2009
Yokota T (15人略) Tsutsui H	Oxidative stress in skeletal muscle impairs mitochondrial respiration and limits exercise capacity in type 2 diabetic mice.	Am J Physiol Heart Circ Physiol	297	1069-1077	2009
Tsutsumi T Ide T Tsutsui H (1人略)	Modulation of the myocardial redox state by vagal nerve stimulation after experimental myocardial infarction	Cardiovasc Res	77	713-721	2008

Wu YW (6 人略) Tsutsui H (1 人略)	Heterogeneous reduction of myocardial oxidative metabolism in patients with ischemic and dilated cardiomyopathy using C-11 acetate PET	Circ J	72	786-792	2008
Makita N (14 人略) Tsutsui H (3 人略)	The E1784K mutation in SCN5A is associated with mixed clinical phenotype of type 3 long QT syndrome	J Clin Invest	118	2219-2229	2008
[室原 豊明] Inden Y Ito R (9 人略) Murohara T	Combined assessment of left ventricular dyssynchrony and contractility by speckled tracking strain imaging: A novel index for predicting responders to cardiac resynchronization therapy.	Heart Rhythm.	7	655-661	2010
Shimano M Ouchi N (3 人略) Murohara T Walsh K	Adiponectin deficiency exacerbates cardiac dysfunction following pressure overload through disruption of an AMPK-dependent angiogenic response.	J. Mol. Cell. Cardiol.	49	210-220	2010
Kondo K Shibata R (7 人略) Murohara T	Impact of a Single Intracoronary Administration of Adiponectin on Myocardial Ischemia/Reperfusion Injury in a Pig Model.	Circ. Cardiovasc. Interv.	3	166-173	2010
Morikawa S Sone T (7人略) Murohara T	Renal protective effects and the prevention of contrast-induced nephropathy by atrial natriuretic peptide.	J. Am. Coll. Cardiol.	53	1040-1046	2009
Unno K Shibata R (8人略) Murohara T	Adiponectin acts as a positive indicator of left ventricular diastolic dysfunction in patients with hypertrophic cardiomyopathy.	Heart		in press	2009
Numaguchi Y Ishii M (5人略) Murohara T	Ablation of Angiotensin IV Receptor Attenuates Hypofibrinolysis via PAI-1 Downregulation and Reduces Occlusive Arterial Thrombosis.	Arterioscler. Thromb. Vasc. Biol.	29	2102-2108	2009

Kitamura T Asai N (9 人略) Murohara T Takahashi M	Regulation of VEGF-mediated angiogenesis by the Akt/PKB substrate Girdin	Nat. Cell Biol	10	329-337	2008
Sugiura T Kondo T (7 人略) Murohara T	Nifedipine improves endothelial function : role of endothelial progenitor cell	Hypertension	52	491-498	2008
Li P Kondo T (4 人略) Murohara T	Role of bradykinin, nitric oxide and angiotensin II type 2 receptor in imidapril-induced angiogenesis	Hypertension	51	252-258	2008
[浅沼 博司] Takahama H Asanuma H (5 人略) Asakura M Takashima S Minamino T (2 人略) Kitakaze M	Histamine H_2 receptor blocker ameliorates development of heart failure in dogs independently of・・・adrenergic receptor blockade	Basic Res Cardiol	105	787-794	2010
Asanuma H Kitakaze M	Hypothetical mechanism of the improvement by adaptive servo-ventilation of the pathophysiology of heart failure associated with sleep-disordered breathing..	Circ J	74	2056-2057	2010
Sasaki H Asanuma H (5 人略) Asakura M (1 人略) Minamino T Takashima S (4 人略) Kitakaze M	Metformin prevents progression of heart failure in dogs: role of AMP-activated protein kinase	Circulation	119	2568-2577	2009
Takahama H Minamino T Asanuma H (7 人略) Asakura M (1 人略) Takashima S (3 人略) Kitakaze M	Prolonged targeting of ischemic/reperfused myocardium by liposomal adenosine augments cardioprotection in rats	J Am Coll Cardiol	53	709-717	2009

Asai M (1 人略) Minamino T Asanuma H (5 人略) Asakura M, Takashima S (1 人略) Kitakaze M	PKA rapidly enhances proteasome assembly and activity in in vivo canine hearts	Journal of molecular and cellular cardiology.	46	452-462	2009
Asanuma H Kitakaze M	Adiponectin is an Important Novel Therapeutic Target in Acute Decompensated Heart Failure – Effect of Carperitide on Plasma Adiponectin Levels –	Circ J	73	2206-2207	2009
Ohara T Kim J Asakura M Asanuma H (5 人略) Kitakaze M	Plasma adiponectin is associated with plasma brain natriuretic peptide and cardiac function in healthy subjects	Hypertens Res	31	825-831	2008
Fujita M Asakura M (4 人略) Asanuma H (6 人略) Kitakaze M	Activation of ecto-5'-nucleotidase in the blood and hearts of patients with chronic heart failure	Journal of Cardiac Failure	14	426-430	2008
[古川 秀比古] Min K Asakura M (7 人略) Asanuma H (1 人略) Minamino T (5 人略) Furukawa H (1 人略) Takashima S (1 人略) Kitakaze M	Identification of genes related to heart failure using global gene expression profiling of human failing myocardium	Biochem. Biophys. Res. Commun.		Feb. 17 [Epub ahead of print]	2009
Nakayama-Hamada M Suzuki A Furukawa H Yamada R Yamamoto K	Citrullinated fibrinogen inhibits thrombin-catalysed fibrin polymerization	Journal of biochemistry	144	393-398	2008

Biochemical and Biophysical Research Communications 393 (2010) 55–60

Contents lists available at ScienceDirect

Biochemical and Biophysical Research Communications

journal homepage: www.elsevier.com/locate/ybbrc

Identification of genes related to heart failure using global gene expression profiling of human failing myocardium

Kyung-Duk Min [a], Masanori Asakura [a,*], Yulin Liao [c], Kenji Nakamaru [d], Hidetoshi Okazaki [a], Tomoko Takahashi [d], Kazunori Fujimoto [d], Shin Ito [a], Ayako Takahashi [a], Hiroshi Asanuma [e], Satoru Yamazaki [b], Tetsuo Minamino [g], Shoji Sanada [a], Osamu Seguchi [a], Atsushi Nakano [a], Yosuke Ando [d], Toshiaki Otsuka [d], Hidehiko Furukawa [d], Tadashi Isomura [f], Seiji Takashima [g], Naoki Mochizuki [b], Masafumi Kitakaze [a]

[a] Department of Cardiovascular Medicine, Osaka, Japan
[b] Research Institute, National Cardiovascular Center, Osaka, Japan
[c] Department of Pathophysiology, Southern Medical University, Guangzhou 510515, China
[d] R&D Division, Daiichi Sankyo Co., Ltd., Tokyo, Japan
[e] Department of Emergency Room Medicine, Kinki University School of Medicine, Sayama, Osaka, Japan
[f] Hayama Heart Center, Hayama, Kanagawa, Japan
[g] Department of Cardiovascular Medicine, Osaka University Graduate School of Medicine, Suita, Osaka, Japan

ARTICLE INFO

Article history:
Received 12 January 2010
Available online 25 January 2010

Keywords:
Gene expression
cDNA microarray
Heart failure
Clinical parameter

ABSTRACT

Although various management methods have been developed for heart failure, it is necessary to investigate the diagnostic or therapeutic targets of heart failure. Accordingly, we have developed different approaches for managing heart failure by using conventional microarray analyses. We analyzed gene expression profiles of myocardial samples from 12 patients with heart failure and constructed datasets of heart failure-associated genes using clinical parameters such as pulmonary artery pressure (PAP) and ejection fraction (EF). From these 12 genes, we selected four genes with high expression levels in the heart, and examined their novelty by performing a literature-based search. In addition, we included four G-protein-coupled receptor (GPCR)-encoding genes, three enzyme-encoding genes, and one ion-channel protein-encoding gene to identify a drug target for heart failure using *in silico* microarray database. After the *in vitro* functional screening using adenovirus transfections of 12 genes into rat cardiomyocytes, we generated gene-targeting mice of five candidate genes, namely, *MYLK3*, *GPR37L1*, *GPR35*, *MMP23*, and *NBC1*. The results revealed that systolic blood pressure differed significantly between *GPR35*-KO and *GPR35*-WT mice as well as between *GPR37L1*-Tg and *GPR37L1*-KO mice. Further, the heart weight/body weight ratio between *MYLK3*-Tg and *MYLK3*-WT mice and between *GPR37L1*-Tg and *GPR37L1*-KO mice differed significantly. Hence, microarray analysis combined with clinical parameters can be an effective method to identify novel therapeutic targets for the prevention or management of heart failure.

Introduction

Heart failure is a multi-factorial condition with increasing prevalence worldwide; further, a significant increase has been observed in the mortality rate and economic impact associated with this condition. In the last 20 years, substantial development of treatment for heart failure, including angiotensin-converting-enzyme inhibitors [1] and beta-blockers [2,3], has greatly improved the prognosis of the patients with heart failure. However, despite these rapid advancements in the management of heart failure, effective treatment of end-stage heart failure without providing ventricular assistance or heart transplantation is still difficult. Investigation of new and unexplored targets for the prevention or treatment of heart failure is warranted. Global gene expression analysis using microarray technique has been used in the last decade to identify biomarkers or drug targets for heart failure [4–10]. Several gene expression signatures of heart failure have been identified by analyzing independent microarray datasets [11,12]. However, most of these analyses did not consider the severity of heart failure. Because the severity of heart failure may quantitatively reflect the expression levels of genes such as the natriuretic

* Corresponding author. Address: Department of Research and Development of Clinical Research, National Cardiovascular Center, 5-7-1 Fujishirodai, Suita, Osaka 565-8565, Japan.
E-mail address: masakura@hsp.ncvc.go.jp (M. Asakura).

0006-291X/$ - see front matter © 2010 Elsevier Inc. All rights reserved.
doi:10.1016/j.bbrc.2010.01.076

peptide-encoding gene, expression analysis combined with the severity of heart failure could be an appropriate method to identify heart failure-related genes. However, microarray analysis of genes expressed in failing myocardium while considering the severity of heart failure has not yet been reported.

Hence, we investigated the genes whose expression level correlated with clinical parameters such as pulmonary artery pressure (PAP), left ventricular ejection fraction (EF), and brain natriuretic peptide (BNP) mRNA level. Using this approach, we identified cardiac myosin light chain kinase as a novel heart failure-related gene [13]. Here, we describe newly identified several genes whose expression correlated with clinical parameters and additional genes encoding G-protein-coupled receptor genes (GPCRs), other enzymes and ion-channel proteins, and performed the functional analysis of these heart failure-related genes. This novel strategy involving the use of clinical parameters might find potential applications for the identification of disease-associated genes that could not be detected using conventional microarray techniques.

Materials and methods

Patient characteristics. We recruited 12 patients (11 males and 1 female) with heart failure and obtained written informed consent from them. The patients were diagnosed with severe chronic heart failure due to various cardiac diseases such as dilated cardiomyopathy and myocardial infarction [13]. The average age of patients was 55 ± 13 years. The plasma level of BNP, which is the best marker for the severity of heart failure, ranged from 80 to 2710 pg/ml. The mean PAP measured using a Swan-Ganz catheter 1–4 weeks before the operation varied between 16 and 59 mmHg. The average of EF determined by echocardiography on the day before the operation was 32.5% ± 12.4%.

Microarray analysis and subsequent in silico functional analysis. RNA was extracted from myocardium samples of 12 heart failure patients who had undergone either Batista or Dor surgeries. RNA samples of non-failing hearts were purchased from Biochain, Inc. Complementary RNA (cRNA) was prepared from RNA samples and hybridized to HG-U95 Affymetrix GeneChip (Affymetrix, US). The expression data were analyzed using Microarray Analysis Suite version 5.0 software. Among all the genes detected on the microarray, we selected the genes whose expression was significantly different in the failing and non-failing myocardial samples ($p < 0.005$). From these genes, we selected genes whose expression was correlated with PAP, EF, and BNP mRNA level, with 0.7 being the cutoff value of the correlation coefficient. The values of PAP, EF, and BNP mRNA level used for the correlation analysis were normalized to their median during the measurements. Subsequently, the functional analysis of datasets was performed using Ingenuity Pathway Analysis (Ingenuity® Systems; www.ingenuity.com), and the biological functions most significant to the dataset were identified.

Cell culture. Cardiomyocytes were harvested before the experiments from 2- to 3-day-old neonatal rats and cultured as described in previous studies [14]. Briefly, primary cardiomyocytes isolated from neonatal rats were grown in Dulbecco's modified Eagle medium/F12 (Gibco) supplemented with 10% fetal calf serum for 72 h, and then cultured in a serum-free condition for 24 h.

Adenovirus generation and transfection. Adenovirus constructs encoding the genes of interest were generated using the ViraPower Adenoviral Expression System (Invitrogen, US) according to the manufacturer's method. Adenovirus vectors were transfected to cultured cardiomyocytes for 12 h according to the published protocol.

In vitro functional analysis of genes. Cultured rat cardiomyocytes were infected by adenovirus vectors. After 24 h, hypertrophic reaction, cell viability, and cellular morphology were assessed. Hypertrophic reaction was determined by estimating the incorporation of [^{3}H]phenylalanine. In brief, [^{3}H]phenylalanine was added to the culture medium at the final concentration of 0.1 μCi/ml, and the cells were incubated for an additional 24 h. Then, the incorporation of [^{3}H]phenylalanine was determined by counting the radioactivity of each sample with a liquid scintillation counter. The viability of cardiomyocytes was evaluated by the Alamar blue assay according to the manufacturer's method. The morphology of cardiomyocytes was evaluated 24 h after adenovirus transfections.

Generation of transgenic and knockout mice. To generate transgenic mice, open reading frame of each gene, namely, *Mylk3*, *Gpr37l1*, or *Nbc1* was amplified from mouse cDNA by PCR, with Sal I site linker on each end, and cloned into Sal I site of alpha-MHC clone 26 vector. Then the DNAs used in the microinjections were released from the vector by digestion with NotI and were microinjected into fertilized eggs of mouse. Founder mice were identified by PCR analysis with appropriate primers. To develop *Gpr37l1* knockout mice, the targeting vector was assembled to replace the exon 1 and 2 by neomycin selection cassete resulting in the absence of *Gpr37l1* protein. W9.5 ES cells were electroporated with linearized targeting vector. ES cell clones with successful homologous recombination was determined by the PCR and subsequent direct sequence. From these targeted ES cells, the chimera mice were bred to C57 BL/6 females to generated F1 and F2 offsprings were obtained. The *Gpr37l1* null mice were determined by PCR genotyping of F2 offsprings. The knockout mice of *Gpr35* and *Mmp23* (*the* mouse ortholog of MMP23B) were purchased from Deltagen, Inc. (California, US).

Invasive blood pressure measurement. The phenotype of the gene-targeted mice was examined. Before sacrificing the mice, their hemodynamic parameters were evaluated. The mice were anesthetized and ventilated, and a Millar catheter was inserted via right carotid artery. The left-ventricular systolic and end-diastolic pressures were measured. Then, the mice were sacrificed and the weight of the whole body and heart was determined.

Statistical analysis. Unpaired Student's *t*-test was used for comparing the two groups. Results are expressed as means ± SEM, and *p* value less than 0.05 was considered statistically significant.

Results

Identification of heart failure-related genes by expression analysis using clinical parameters

We performed microarray analysis of the genes expressed in failing myocardium obtained from 12 patients with heart failure and the genes expressed in non-failing myocardium from two normal objects whose characteristics were reported in the previous study [13]. Although all patients were diagnosed with chronic heart failure, the plasma BNP level, which is an index of the severity of heart failure, ranged from 80 to 2710 pg/ml, suggesting that the severity of heart failure varied extensively among the patients. This marked difference in the severity of heart failure reflects the fact that the gene expression patterns in the 12 patients were not uniform, as shown in Fig. 1A. Thus, we analyzed gene expression profiles of failing myocardium using clinical parameters representing the severity of heart failure. We identified 166 and 194 genes whose expressions were correlated with PAP and BNP mRNA level, respectively (Fig. 1B and Supplementary Tables S1, S2). Among these, 49 genes correlated with both PAP and BNP mRNA level (Fig. 1C). The expression of only two genes, namely, *FMO2* and *LMAN1L*, correlated with the EF. We investigated the functional categories of these genes by performing Ingenuity Pathway Analysis. The number of genes in each group, functional categories, and

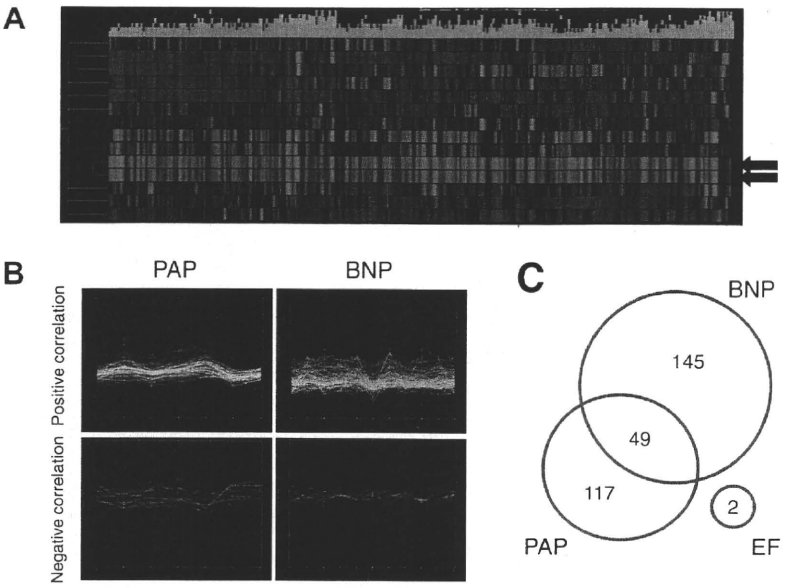

Fig. 1. The gene expression profile of human failing or non-failing myocardium. Gene expression levels of myocardial samples from 12 patients with severe heart failure and from two normals were analyzed using microarray. (A) Heat maps showing the genes with differential expression between the 12 failing myocardial samples and the two non-failing myocardial samples. Red color indicates upregulated gene expression. Green color indicates downregulated gene expression. Arrows indicate non-failing samples. (B) Expression profile of positively or negatively correlated genes to pulmonary artery pressure (PAP) or brain natriuretic peptide (BNP) mRNA level ($r > 0.7$). (C) Venn diagram of genes correlated with PAP, BNP, and ejection fraction.

Table 1
Datasets of genes whose expressions were correlated to clinical parameters.

	PAP	EF	BNP mRNA level
Positive correlation			
Number	124	1	175
Function	Cardiovascular system development and function Cell death	–	Cardiovascular system development and function Cell cycle
Representative genes	*ARNT, MYOCD, SMARCA4* *BGN, CFLAR, EEF2, MTPN*	*LMAN1L*	*BTG1, NPPA, NPPB, SERPNF1* *CKS1B, DDR2, FCGR2B, FN1*
Negative correlation			
Number	42	1	19
Function	Skeletal and muscular system development and function Cellular assembly and organization	–	Skeletal and muscular system development and function Cellular assembly and organization
Representative genes	*PIK3R1, PRKAR1A, SLMAP* *C19ORF20, RAB9A, SYNGAP1, TTN*	*FMO2*	*ACTC1, RBBP4, TTN*

The function of gene sets was analyzed by Ingenuity Pathway Analysis.
PAP, pulmonary artery pressure; EF, ejection fraction; BNP, brain natriuretic peptide.

representative genes are shown in Table 1. Interestingly, both gene sets correlated positively with PAP and BNP mRNA level were most associated with the same functional category of "cardiovascular system development and function", although the included genes were different. Similarly, the gene sets correlated negatively with both PAP and BNP mRNA level had most association with common functional categories of "skeletal and muscular system development and function" and "cellular assembly and organization".

Selection of 12 genes for in vitro screening

Among the genes selected using clinical parameters, we selected those genes that showed high expression levels in the heart by performing microarray analysis. On the basis of their novelty determined by a literature-based search, we selected four genes for further investigation (Table 2). Concurrently, to identify possible drug targets, we included four orphan GPCRs and four additional genes (three enzyme-encoding genes and one ion-channel protein-encoding gene) in the further analysis. The *RHOQ* and *STK38* genes were selected based on their correlation with BNP mRNA level and PAP, respectively. *GPR161* and *NBC1* were selected owing to their high expression level in the heart. *GPR37L1*, *GPR35*, *F2RL2*, and *MMP23B* were selected because of their high expression level in the heart, and their association with the cardiac diseases-related genes listed in the database was determined by *in silico* analysis.

Functional analysis of genes on the basis of adenovirus-mediated overexpression of proteins in neonatal rat cardiomyocytes

To determine which of the selected genes were associated with the physiological functions of the heart, we first generated adenovirus vectors for each gene listed in Table 2 and transfected these vectors into neonatal rat cardiomyocytes. Next, we evaluated the hypertrophic reaction, viability, and morphology of the transfected cardiomyocytes. Among the 12 selected genes, three adenovirus-mediated genes decreased the incorporation of [^{3}H]phenylalanine in neonatal rat cardiomyocytes (Table 2); the expression of one

Table 2
In vitro functional screening of the 12 candidate genes.

Probe set ID	Gene symbol	Gene name	Criteria for selection	*p* value	[^{3}H]PA intake	Fluorescence of Alamar blue	Cellular morphology
Genes relevant to clinical parameters							
75678_at	*MYLK3*	Myosin light chain kinase 3	Correlation with PAP ($r = 0.792$)	0.00262	No change	No change	Spiking
49333_at	*XPR1*	Xenotropic and polytropic retrovirus receptor	Correlation with PAP ($r = 0.765$), GPCR, change in CHF	0.00045	No change	No change	No change
38435_at	*PRDX4*	Peroxiredoxin 4	Correlation with BNP ($r = 0.863$)	0.00024	Increased	Decreased	No change
45314_at	*SMOC2*	SPARC related modular calcium binding 2	Correlation with both PAP and BNP ($r = 0.715$ and 0.758, respectively)	0.00444	No change	No change	No change
Genes encoding orphan GPCRs							
35544_at	*GPR37L1*	G-protein-coupled receptor 37 like 1	Orphan GPCR, downregulated in CVD	>0.005	Decreased	Decreased	Apoptosis
31700_at	*GPR35*	G-protein-coupled receptor 35	Orphan GPCR, upregulated in MI	0.00216	Decreased	Decreased	Hypertrophy
45204_at	*F2RL2*	Coagulation factor II (thrombin) receptor-like 2	GPCR, change in CVD	>0.005	Increased	No change	No change
40299_at	*GPR161*	G-protein-coupled receptor 161	GPCR, expression in heart	>0.005	Decreased	Decreased	No change
Genes encoding interesting enzymes or ion-channels							
38950_at	*MMP23B*	Matrix metallopeptidase 23B	Family of MMP, change in CHF	>0.005	No change	Decreased	No change
35285_at	*NBC1*	Na^+–HCO^{3-} cotransporter 1	Expression in heart	>0.005	No change	Decreased	No change
87788_at	*RHOQ*	Ras homolog gene family, member Q	Expression in DCM, correlation with BNP ($r = 0.711$)	>0.005	No change	No change	No change
78801_at	*STK38*	Serine/threonine kinase 38	Kinase activity, correlation with PAP ($r = 0.736$)	>0.005	No change	No change	No change

PAP, pulmonary artery pressure; GPCR, G-protein-coupled receptor; CHF, congestive heart failure; BNP, brain natriuretic peptide; CVD, cardiovascular disease; MI, myocardial infarction; DCM, dilated cardiomyopathy; PA, phenylalanine. *p* value indicates the significance of the difference between the gene expression level of failing and non-failing myocardium.

gene promoted [^{3}H]phenylalanine incorporation; and the overexpression of six genes lowered the viability of cardiomyocytes, which was evaluated by Alamar blue assay. We also evaluated the phenotype of transfected cardiomyocytes. Unlike control cells, *MYLK3*-adenovirus-transfected cardiomyocytes were spike shaped. The overexpression of *GPR37L1* induced apoptosis of cardiomyocytes. The transfection of *NBC1*-adenoviral vectors modified the beating rate of cardiomyocytes (data not shown). Then, we analyzed each gene that encoded a distinct cardiomyocyte phenotype by developing gene-targeted mouse models.

In vivo analysis using transgenic and knockout mice

To study the *in vivo* role of the selected genes, we developed genetically modified mice: three transgenic (Tg) mice for *Mylk3*, *Gpr37l1*, or *Nbc1* and three knockout (KO) mice for *Gpr37l1*, *Gpr35*, or *Mmp23*. We estimated hemodynamic parameters using Miller catheter and the heart weight (HW)/body weight (BW). As shown in Fig. 2A, we found that the blood pressure of *Gpr37l1*-KO mice was significantly higher than that of *Gpr37l1*-Tg mice by 61.7 mmHg ($p < 0.01$). Further, the blood pressure of *Gpr35*-KO mice was higher than that of wild type (WT) littermate by 37.5 mmHg ($p < 0.01$). Overexpression with or knockout of *Mylk3*, *Mmp23*, or *Nbc1* did not result in a significant change in the systolic blood pressure. The HW/BW of *Mylk3*-Tg mice was lower than that of *Mylk3*-WT mice (Fig. 2B). The HW/BW was higher in *Gpr37l1*-KO mice than in *Gpr37l1*-Tg mice. The HW/BW in mice with *Nbc1*, *Gpr35*, or *Mmp23* manipulations did not show any difference. These data showed that modification of *Gpr37l1*, *Gpr35*, or *Mylk3* can produce a distinct cardiovascular phenotype *in vivo*.

Discussion

The present study identified heart failure-related genes using a novel strategy that was different from the conventional microarray analysis approach. Firstly, we constructed global gene expression profiles to analyze the gene expression in 12 human samples of failing myocardium and two samples of non-failing myocardium. Secondly, we prepared datasets of heart failure-related genes associated with the severity of heart failure; this approach is unique to our study and has not been published before. Thirdly, we selected four genes from these datasets by microarray analysis and a literature-based search. We also included four orphan GPCR genes and four other genes with high expression in the heart as possible drug targets for heart failure treatment. Fourthly, we screened the *in vitro* functions of these 12 genes by achieving adenovirus-mediated overexpression of these genes in rat cardiomyocytes. Finally, we generated gene-targeted mouse models of the five selected genes and screened the *in vivo* functions of these genes. Our novel strategy using a microarray analysis revealed three potential targets, namely, *MYLK3*, *GPR37L1*, and *GPR35* for diagnosing and managing heart failure.

End-stage heart failure caused by a variety of cardiovascular diseases including hypertension, cardiomyopathy, and ischemic heart disease features a common phenotype of reduced cardiac function and dilated cardiac chamber. This result strongly suggested the existence of common genes during the development of heart failure, including the genes encoding natriuretic peptides. To identify novel diagnostic or therapeutic targets for heart failure, such as natriuretic peptides, several microarray analyses of genes expressed in failing myocardium have been performed in the last decade by comparing the gene expression levels between different pairs of samples, such as non-failing versus failing hearts [4–6], failing hearts before versus after placement of left-ventricular assisting device [7,8], hypertrophic versus failing hearts [9], ischemic versus non-ischemic hearts [10]. However, the severity of heart failure is not fixed, but varies from mild to severe heart failure in these studies. To identify the therapeutic targets for heart failure effectively, we believe that it is important to consider the severity of heart failure with microarray data analysis. In this study, we prepared new datasets of heart failure-associated genes that were selected from gene expression profiles of 12 human failing myocardial samples using clinical parameters. A number of genes were associated with PAP, which is an index for the severity of heart failure, whereas only two genes correlated with EF, which is an index for cardiac contractility. This result implies that the stress caused to the heart, and not the ability of cardiac contraction, regulates gene expression in heart failure. We also selected heart failure-related genes whose expression correlated to

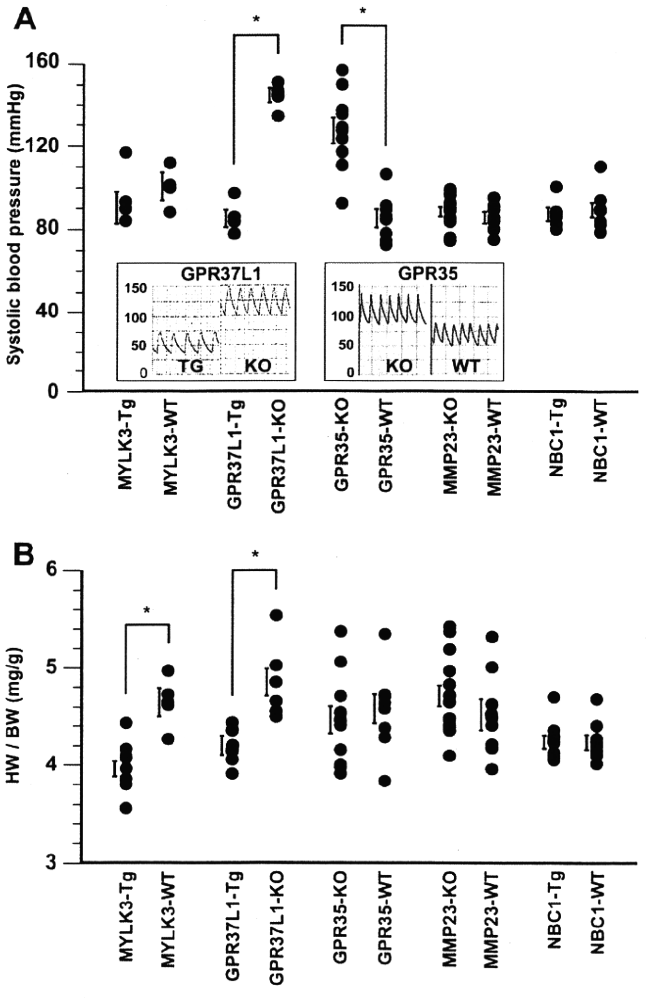

Fig. 2. *In vivo* functional analysis using gene-targeting mice of the *Mylk3*, *Gpr37l1*, *Gpr35*, *Mmp23*, and *Nbc1* genes. Blood pressure and heart weight (HW)/body weight (BW) of transgenic (Tg), knockout (KO) and their wild type (WT) littermate mice of each gene were investigated. Values are means ± SEM. $^*p < 0.01$. (A) Systolic blood pressure measured using Millar catheter inserted via right carotid artery. The monitoring chart shows representative data of *Gpr37l1*- and *Gpr35*-manipulated mice. (B) HW/BW ratio of each gene-targeting mouse.

the BNP mRNA level, which is the best known indicator of heart failure. The approach used in our study can help in efficient identification of the diagnostic or therapeutic targets for heart failure rather than only comparing two types of samples such as failing versus non-failing myocardium. Among the genes from these new datasets, we focused on the genes exhibiting high expression in heart tissues and finally selected four genes for performing the screening of functional analysis *in vitro*. The expression level of *MYLK3* gene was highly correlated to PAP, and this gene was detected only in the heart tissue. Recently, we reported that *MYLK3* plays a crucial role in sarcomere assembly via phosphorylation of myosin regulatory light chain 2V (MLC2v) [13]. We also showed that the knockdown of *MYLK3* by using a morpholino oligo caused immature sarcomere formation leading to ventricular dilation in zebrafish. These results indicate that *MYLK3* is strongly associated with the pathophysiology of heart failure. Chan et al. also reported that MYLK3 phosphorylates MLC2v and regulates sarcomere organization [15]. These reports affirm the reliability of our original strategy that involves the microarray analysis of failing myocardium. Among these genes, most genes including *XPR1*, *PRDX4*, and *SMOC2* have not been reported to link with cardiovascular phenotypes and were not included in many gene expression profiles published previously.

Next, we performed *in vivo* functional analysis of five selected genes, and we found that gene-targeted mouse models of *Mylk3*, *Gpr37l1*, or *Gpr35* showed the cardiovascular phenotype. As described above, *Mylk3* plays a crucial role in failing heart. In this study, we identified two GPCRs, namely, *Gpr37l1* and *Gpr35*, whose modification affects systolic blood pressure or HW/BW. To our knowledge, this is the first report about the role of these genes in cardiovascular system.

GPCRs constitute one of the largest protein families, but many GPCRs remain to be orphaned. GPR35 is now known to have some ligands such as kynurenic acid (KYNA) [16], zaprinast [17], and 5-nitro-2-(3-phenylpropylamino) benzoic acid [18]. These agonists mobilize intracellular calcium concentration. Therefore, lowering systolic blood pressure in *Gpr35*-KO mice can be induced by modulating calcium release from calcium-storing organelles. Among the three agonists, only KYNA is produced endogenously as a metabolite of tryptophan. Although GPR35 gene expression is supposed to be specific to immune cells and gastrointestinal tract, we found that GPR35 gene expression increased in failing myocardium. In an inflammatory state, interferon γ induces idolemine 2,3-dioxygenase, a rate-limiting enzyme involved in tryptophan degradation, resulting in a substantial increase in KYNA. Inflammation is thought to be involved in the pathogenesis of dilated cardiomyopathy as well as myocardial infarction. Hence there is a possibility that a KYNA-GPR35 signaling plays a role in the pathogenesis of cardiovascular diseases.

Unlike GPR35, GPR37L1 is still orphaned. However, we found that *Gpr37l1*-KO mice showed significant high blood pressure and high HW/BW as compared to Tg mice, which implies the existence of cardiovascular-related function of *Gpr37l1*. Identification of the ligand and the function of this orphan receptor are awaited.

Although no significant phenotype was observed in *Mmp23* and *Nbc1*-Tg mice, we have been investigating their cardiac function in pathological condition such as myocardial infarction or hypertension and determined their detrimental effect on heart failure (data not shown).

In the present study, we determined 12 novel heart failure-related genes by integrating an original method with parameters that indicated disease severity. Further, we assessed these possible targets of drug discovery. *MYLK3*, *GPR37L1*, and *GPR35* were the newly identified targets that play an interesting role in the cardiovascular system.

Acknowledgments

This study was supported by Grant-in-Aid for Scientific Research (C) in Japan Society for the Promotion of Science; a grant from Human Genome Tissue Engineering and Food Biotechnology in Health and Labor Science Research from the Ministry of Health, Labor, and Welfare, Japan; and a grant from Japan Cardiovascular Research Foundation.

Appendix A. Supplementary data

Supplementary data associated with this article can be found, in the online version, at doi:10.1016/j.bbrc.2010.01.076.

References

[1] Effect of enalapril on survival in patients with reduced left ventricular ejection fractions and congestive heart failure. The SOLVD Investigators, N. Engl. J. Med. 325 (1991) 293–302.
[2] Effect of metoprolol CR/XL in chronic heart failure: metoprolol CR/XL randomised intervention trial in congestive heart failure (MERIT-HF), Lancet 353 (1999) 2001–2007.

[3] M. Packer, M.R. Bristow, J.N. Cohn, W.S. Colucci, M.B. Fowler, E.M. Gilbert, N.H. Shusterman, The effect of carvedilol on morbidity and mortality in patients with chronic heart failure. U.S. Carvedilol Heart Failure Study Group, N. Engl. J. Med. 334 (1996) 1349–1355.
[4] J. Yang, C.S. Moravec, M.A. Sussman, N.R. DiPaola, D. Fu, L. Hawthorn, C.A. Mitchell, J.B. Young, G.S. Francis, P.M. McCarthy, M. Bond, Decreased SLIM1 expression and increased gelsolin expression in failing human hearts measured by high-density oligonucleotide arrays, Circulation 102 (2000) 3046–3052.
[5] J.D. Barrans, P.D. Allen, D. Stamatiou, V.J. Dzau, C.C. Liew, Global gene expression profiling of end-stage dilated cardiomyopathy using a human cardiovascular-based cDNA microarray, Am. J. Pathol. 160 (2002) 2035–2043.
[6] F.L. Tan, C.S. Moravec, J. Li, C. Apperson-Hansen, P.M. McCarthy, J.B. Young, M. Bond, The gene expression fingerprint of human heart failure, Proc. Natl. Acad. Sci. USA 99 (2002) 11387–11392.
[7] B.C. Blaxall, B.M. Tschannen-Moran, C.A. Milano, W.J. Koch, Differential gene expression and genomic patient stratification following left ventricular assist device support, J. Am. Coll. Cardiol. 41 (2003) 1096–1106.
[8] J.L. Hall, E.J. Birks, S. Grindle, M.E. Cullen, P.J. Barton, J.E. Rider, S. Lee, S. Harwalker, A. Mariash, N. Adhikari, N.J. Charles, L.E. Felkin, S. Polster, R.S. George, L.W. Miller, M.H. Yacoub, Molecular signature of recovery following combination left ventricular assist device (LVAD) support and pharmacologic therapy, Eur. Heart J. 28 (2007) 613–627.
[9] J. Rysa, H. Leskinen, M. Ilves, H. Ruskoaho, Distinct upregulation of extracellular matrix genes in transition from hypertrophy to hypertensive heart failure, Hypertension 45 (2005) 927–933.
[10] M.M. Kittleson, S.Q. Ye, R.A. Irizarry, K.M. Minhas, G. Edness, J.V. Conte, G. Parmigiani, L.W. Miller, Y. Chen, J.L. Hall, J.G. Garcia, J.M. Hare, Identification of a gene expression profile that differentiates between ischemic and nonischemic cardiomyopathy, Circulation 110 (2004) 3444–3451.
[11] A.S. Barth, R. Kuner, A. Buness, M. Ruschhaupt, S. Merk, L. Zwermann, S. Kaab, E. Kreuzer, G. Steinbeck, U. Mansmann, A. Poustka, M. Nabauer, H. Sultmann, Identification of a common gene expression signature in dilated cardiomyopathy across independent microarray studies, J. Am. Coll. Cardiol. 48 (2006) 1610–1617.
[12] M. Asakura, M. Kitakaze, Global gene expression profiling in the failing myocardium, Circ. J. 73 (2009) 1568–1576.
[13] O. Seguchi, S. Takashima, S. Yamazaki, M. Asakura, Y. Asano, Y. Shintani, M. Wakeno, T. Minamino, H. Kondo, H. Furukawa, K. Nakamaru, A. Naito, T. Takahashi, T. Ohtsuka, K. Kawakami, T. Isomura, S. Kitamura, H. Tomoike, N. Mochizuki, M. Kitakaze, A cardiac myosin light chain kinase regulates sarcomere assembly in the vertebrate heart, J. Clin. Invest. 117 (2007) 2812–2824.
[14] M. Asakura, M. Kitakaze, S. Takashima, Y. Liao, F. Ishikura, T. Yoshinaka, H. Ohmoto, K. Node, K. Yoshino, H. Ishiguro, H. Asanuma, S. Sanada, Y. Matsumura, H. Takeda, S. Beppu, M. Tada, M. Hori, S. Higashiyama, Cardiac hypertrophy is inhibited by antagonism of ADAM12 processing of HB-EGF: metalloproteinase inhibitors as a new therapy, Nat. Med. 8 (2002) 35–40.
[15] J.Y. Chan, M. Takeda, L.E. Briggs, M.L. Graham, J.T. Lu, N. Horikoshi, E.O. Weinberg, H. Aoki, N. Sato, K.R. Chien, H. Kasahara, Identification of cardiac-specific myosin light chain kinase, Circ. Res. 102 (2008) 571–580.
[16] J. Wang, N. Simonavicius, X. Wu, G. Swaminath, J. Reagan, H. Tian, L. Ling, Kynurenic acid as a ligand for orphan G protein-coupled receptor GPR35, J. Biol. Chem. 281 (2006) 22021–22028.
[17] Y. Taniguchi, H. Tonai-Kachi, K. Shinjo, Zaprinast, a well-known cyclic guanosine monophosphate-specific phosphodiesterase inhibitor, is an agonist for GPR35, FEBS Lett. 580 (2006) 5003–5008.
[18] Y. Taniguchi, H. Tonai-Kachi, K. Shinjo, 5-Nitro-2-(3-phenylpropylamino)-benzoic acid is a GPR35 agonist, Pharmacology 82 (2008) 245–249.

Left Atrial Volume Combined With Atrial Pump Function Identifies Hypertensive Patients With a History of Paroxysmal Atrial Fibrillation

Norihisa Toh, Hideaki Kanzaki, Satoshi Nakatani, Takahiro Ohara, Jiyoong Kim, Kengo F. Kusano, Kazuhiko Hashimura, Tohru Ohe, Hiroshi Ito, Masafumi Kitakaze

Abstract—Identifying patients at high risk for the occurrence of atrial fibrillation is one means by which subsequent thromboembolic complications may be prevented. Left atrial enlargement is associated with progression of atrial remodeling, which is a substrate for atrial fibrillation, but impaired atrial pump function is also another aspect of the remodeling. Our objective was to differentiate patients with a history of paroxysmal atrial fibrillation using echocardiography. We studied 280 hypertensive patients (age: 66±7 years; left ventricular ejection fraction: 65±8%), including 140 consecutive patients with paroxysmal atrial fibrillation and 140 age- and sex-matched control subjects. Left atrial volume was measured using the modified Simpson method at both left ventricular end systole and preatrial contraction and was indexed to body surface area. Peak late-diastolic mitral annular velocity was measured during atrial contraction using pulsed tissue Doppler imaging as an atrial pump function. Left atrial volume index measured at left ventricular end systole had a 74% diagnostic accuracy and a 71% positive predictive value for identifying patients with paroxysmal atrial fibrillation; these values for the ratio of left atrial volume index at left ventricular end systole to the peak late-diastolic mitral annular velocity were 82% and 81%, respectively, and those for the ratio of left atrial volume index at preatrial contraction to the peak late-diastolic mitral annular velocity were 86% and 90%, respectively. In conclusion, left atrial size combined with atrial pump function enabled a more accurate diagnosis of a history of paroxysmal atrial fibrillation than conventional parameters. (***Hypertension.* 2010;55:1150-1156.**)

Key Words: hypertension ■ echocardiography ■ atrial fibrillation ■ left atrium ■ remodeling

Atrial fibrillation (AF) is not generally life threatening but is considered to be the most common cause of ischemic stroke, which often yields serious complications because of acute occlusion of intracranial arteries without collateral circulation. The incidence of stroke is increased by ≈5-fold in the presence of nonvalvular AF.[1–5] Moreover, recent studies have demonstrated that stroke risk is no less in patients with paroxysmal AF (PAF) than in those with persistent AF.[6] Therefore, it is crucial to identify patients who have PAF in order to prevent subsequent thromboembolic complications, especially in patients with hypertension, which is a major etiologic factor associated with both AF and stroke.[7–9]

Left atrial (LA) enlargement associated with the progression of atrial structural remodeling plays a key role in the initiation and maintenance of AF.[10,11] The most recent recommendations for echocardiographic chamber quantification indicate that LA volume (LAV) provides an accurate measurement of asymmetrical remodeling of the LA chamber.[12] LAV is increased in patients with PAF[13] and is also an important predictor of cardiovascular outcome, including the occurrence of AF,[14] supporting the concept that LAV is a hallmark of atrial remodeling.

In patients with PAF, Doppler transmitral flow velocity and tissue Doppler imaging (TDI)–derived mitral annulus velocity during atrial contraction, which are considered to reflect atrial pump function,[15–20] have been reported to be decreased compared with those in control subjects.[13,16,21] According to the Frank-Starling law, atrial pump function is also enhanced with an increase in LAV; however, excessive LA enlargement leads to atrial dysfunction.[22,23] Accordingly, we hypothesized that adding information on atrial pump function may provide a better marker of atrial remodeling.

In the present study, we aimed to differentiate patients with a history of PAF among those with hypertension more accurately by means of LAV combined with atrial pump function.

Methods

Study Population

Patients referred to our laboratory were classified into the PAF group if they met the following criteria: (1) ≥1 episode of self-terminating

Received June 18, 2009; first decision July 6, 2009; revision accepted March 8, 2010.

From the Cardiovascular Division of Medicine (N.T., H.K., S.N., T.O., J.K., K.H., M.K.), National Cardiovascular Center, Osaka, Japan; Department of Cardiovascular Medicine (K.F.K., H.I.), Okayama University Graduate School of Medicine, Dentistry, and Pharmaceutical Sciences, Okayama, Japan; Department of Cardiology (T.O.), Sakakibara Heart Institute of Okayama, Okayama, Japan.

Correspondence to Hideaki Kanzaki, Cardiovascular Division of Medicine, National Cardiovascular Center, 5-7-1 Fujishiro-dai, Suita, Osaka 565-8565, Japan. E-mail kanzakih@hsp.ncvc.go.jp

***Hypertension* is available at http://hyper.ahajournals.org** **DOI: 10.1161/HYPERTENSIONAHA.109.137760**

PAF documented by a 12-lead ECG, 24-hour Holter monitoring, or continuous monitoring during hospitalization without taking any antiarrhythmic drugs and having been free from arrhythmic episodes for >1 week before undergoing echocardiography; (2) hypertension (systolic blood pressure ≥140 mm Hg and/or diastolic blood pressure ≥90 mm Hg or treatment for hypertension); (3) less than moderate mitral regurgitation; (4) sinus rhythm during echocardiography; (5) no medical history of other arrhythmias (including persistent AF), valvular heart disease (including mitral annular calcification), heart failure, ischemic heart disease, cardiomyopathy, cardiac surgery, thyroid disease, or pulmonary disease; and (6) age between 40 and 80 years.

Control subjects were recruited from a clinical health examination in Arita, Japan. All of the attendees underwent a formal medical history interview, ECG, and physical and laboratory examinations. Blood pressure was measured at each of ≥2 visits to the office, and the average of ≥2 seated blood pressures was used according to established recommendations.[24] Of the attendees who also underwent echocardiography, age- and sex-matched subjects who met criteria 2 through 6 were classified as the control group. The study was approved by the institutional review board, and the study was conducted in accordance with the ethical principles of the Declaration of Helsinki. All of the subjects provided informed consent.

Echocardiography

All of the echocardiographic studies were performed with either a Vivid 7 Dimension (GE Healthcare) or Aplio XV (Toshiba Medical Systems) ultrasound system. Cardiac chamber size, left ventricular (LV) ejection fraction (LVEF), LV mass, and LA dimension were evaluated according to the recommendations of the American Society of Echocardiography.[12] LAV was measured using the biplane modified Simpson's method at the ventricular end-systolic frame just before the mitral valve opening from apical 4- and 2-chamber views. Strictly speaking, however, LA does not contract from the size of LAV at ventricular end systole. Thus, preatrial contraction LAV (LAV_{preA}) was also obtained from the last frame just before mitral valve reopening. Active LA emptying fraction (active LAEF) was calculated by the following formula: $(LAV_{preA}-LAV_{min})/LAV_{preA}\times100\%$, where LAV_{min} is the minimal LAV at atrial end systole. All of the LAVs were indexed to body surface area as LAVi, $LAVi_{preA}$, and $LAVi_{min}$, respectively. LV mass was also indexed to body surface area (LV mass index). LV hypertrophy was defined as LV mass index >104 g/m^2 in women and >116 g/m^2 in men.[25]

The sample volume of pulsed-wave Doppler imaging was placed at the tip level of the mitral leaflets in the apical 4-chamber view. Then the peak mitral inflow early diastolic and atrial filling (E and A) velocities and the E-wave deceleration time were obtained. The sample volume of the pulsed TDI was placed at the septal and lateral margins of the mitral annulus. Peak early and late-diastolic mitral annular velocities were measured, and then the average values of septal and lateral velocities were used as Ea and Aa, respectively. E/Ea was calculated as a surrogate for the LV filling pressure.[26]

Statistical Analysis

Data are expressed as mean±SD. An ANOVA was performed to test for statistically significant differences between 2 unpaired mean values, and categorical data and percentage frequencies were analyzed by the χ^2 test. Correlations were determined with Pearson product moment correlation analysis. Receiver operating characteristic (ROC) curves were constructed to determine the optimal sensitivity and specificity. The area under the curve (AUC) was calculated to assess the overall performance of various variables for the detection of PAF. Univariate and multivariate logistic regression analyses were performed to characterize diagnostic factors of a history of PAF. Variables considered included age, sex, body weight, LV hypertrophy, E/Ea, and diabetes mellitus. A scatter diagram was used to illustrate the relationship between LA size and LA pump function in each patient. A straight line was drawn passing through the origin to discriminate the best between the PAF and control groups, and another line was drawn to establish the boundary above which spots belonging to the PAF group existed. The slope indicates the ratio of LA size to LA pump function: the former corresponds to the optimal cutoff value from the ROC analysis and the latter is the minimum of the ratios of the PAF group. Most statistical tests were performed with SPSS version 12.0 (SPSS Inc). The calculation and comparison of AUC values and the logistic regression analyses were performed with Stata SE version 8.2 (Stata Corp). A P value <0.05 was considered to be statistically significant. The statistical power of the present study was finally calculated.

Forty subjects were randomly selected from each group and analyzed blindly by 2 authors (N.T. and H.K.) to assess reproducibility. The interobserver and intraobserver variabilities were, respectively, 4.0% and 3.8% for LAV, 4.2% and 4.2% for LAV_{preA}, 12.3% and 9.9% for LAV_{min}, 4.4% and 4.1% for peak A velocity, 3.6% and 3.5% for septal Aa, and 4.0% and 3.7% for lateral Aa.

Table 1. Clinical Characteristics of the Study Population

Variable	Control Group (n=140)	PAF Group (n=140)
Age, y	66±7	66±8
Women, %	47	47
Height, cm	158±9	160±10
Weight, kg	58±10	60±10
Body surface area, m^2	1.59±0.17	1.60±0.26
Body mass index, kg/m^2	23.2±3.3	23.6±3.0
Systolic blood pressure, mm Hg	140±18	137±16
Diastolic blood pressure, mm Hg	82±10	80±11
Diabetes mellitus, %	17	21
Hyperlipidemia, %	46	47
Smoking, %	31	23
Concomitant cardiovascular therapies		
ACE inhibitors, %	7	5
ARBs, %	30	32
β-Blockers, %	18	27
Calcium channel blockers, %	32	37

Values are expressed as mean±SD unless otherwise specified. ACE indicates angiotensin-converting enzyme; ARB, angiotensin II receptor blockers. No significant differences were found between groups.

Results

Clinical and Echocardiographic Characteristics

A total of 280 subjects with hypertension (mean age: 66±7 years; range: 40 to 80 years; 148 men; LVEF: 65±8%) were enrolled in the present study. There were no significant differences in clinical parameters or the use of antihypertensive drugs between the 140 control and 140 PAF subjects (Table 1). The median time interval between the first PAF episode and this examination was 2.0 years (25th to 75th percentile: 0.2 to 7.0 years), and 62% of the patients with PAF were symptomatic. Echocardiographic characteristics are depicted in Table 2. No significant group differences were found for the following parameters: LV end-diastolic diameter, LV end-systolic diameter, and LVEF. LV mass index, LA dimension, and indices related to the LAV were significantly increased in the PAF group compared with those in the control group, whereas active LAEF was decreased in the PAF group. The prevalences of LV hypertrophy were 45% in the PAF group (37 women and 25 men) and 28% in the control group (18 women and 21 men). The E-wave decel-

Table 2. Echocardiographic Characteristics of the Study Population

Variable	Control Group (n=140)	PAF Group (n=140)	*P*
LV end-diastolic dimension, mm	47±5	46±5	0.114
LV end-systolic dimension, mm	28±5	28±5	0.445
LVEF, %	65±8	65±8	0.839
LV mass index, g/m^2	100±20	112±27	<0.001
LA dimension, mm	38±5	43±5	<0.001
LAVi, ml/m^2	30±7	42±12	<0.001
$LAVi_{preA}$, ml/m^2	21±6	32±10	<0.001
$LAVi_{min}$, ml/m^2	14±4	25±10	<0.001
Active LAEF, %	34±8	23±10	<0.001
Peak E velocity, cm/s	64±15	70±19	0.007
Peak A velocity, cm/s	80±18	67±21	<0.001
E/A	0.85±0.24	1.18±0.67	<0.001
E-wave deceleration time, ms	233±44	224±49	0.069
Ea, cm/s	7.5±1.9	6.8±1.9	<0.001
Aa, cm/s	11.1±2.3	7.7±2.6	<0.001
E/Ea	9.0±2.5	11.1±4.3	<0.001
LAVi/A, mL · m^{-2}/cm · s^{-1}	0.39±0.11	0.72±0.41	<0.001
LAVi/Aa, mL · m^{-2}/cm · s^{-1}	2.9±1.0	6.8±5.1	<0.001
$LAVi_{preA}$/active LAEF	0.64±0.28	1.96±2.23	<0.001
$LAVi_{preA}$/A, mL · m^{-2}/cm · s^{-1}	0.27±0.08	0.55±0.36	<0.001
$LAVi_{preA}$/Aa, mL · m^{-2}/cm · s^{-1}	1.9±0.4	5.3±4.3	<0.001

Values are expressed as mean±SD.

eration time was comparable, but peak E velocity was significantly greater, and peak A velocity was less in the PAF group than in the control group. The Ea and Aa were lower in the PAF group than in the control group. E/Ea was greater in the PAF group than in the control group.

The following correlations were found: (1) LAVi and $LAVi_{preA}$ were correlated with E/Ea (LAVi: r=0.418, P<0.001; $LAVi_{preA}$: r=0.416, P<0.001); (2) LAVi and $LAVi_{preA}$ were correlated with LV mass index (LAVi: r=0.440, P<0.001; $LAVi_{preA}$: r=0.459, P<0.001); (3) LAVi was strongly correlated with the $LAVi_{preA}$ (r=0.916; P<0.001); (4) Aa was correlated well with active LAEF (r=0.755; P<0.001) and this correlation was still observed in patients with severely enlarged LA (r=0.775; P<0.001), which is defined as LAVi >40 mL/m^2 in the recommendations[12]; and (5) LAVi/Aa and $LAVi_{preA}$/Aa were correlated with the time interval between the first PAF episode and this examination (LAVi/Aa: r=0.267, P=0.012; $LAVi_{preA}$/Aa: r=0.275, P=0.009).

Echocardiographic Detection of PAF Among Hypertensive Patients

Various parameters, listed in Table 3, were examined using ROC analysis. $LAVi_{preA}$/Aa was best for detecting patients with a history of PAF considering the AUC. The AUC of $LAVi_{preA}$/Aa was statistically greater than those of the $LAVi_{preA}$/A, $LAVi_{preA}$/active LAEF, LAVi/Aa, and LAVi values (P=0.024, P=0.003, P<0.001, and P<0.001, respectively). Although the statistical power calculated was 76% because of the limited number of subjects, statistically significant differences were found between the $LAVi_{preA}$/Aa ratio and other parameters. The ROC curves for the $LAVi_{preA}$/Aa, LAVi/Aa, LAVi, and LA dimension are shown in Figure 1.

Table 3. AUCs for Echocardiographic Variables

Variable	AUC	SE	95% CI
LA dimension	0.733	0.030	0.675 to 0.791
LAVi	0.820	0.024	0.772 to 0.868
$LAVi_{preA}$	0.861	0.022	0.819 to 0.904
LAVi/A	0.852	0.023	0.807 to 0.898
LAVi/Aa	0.884	0.019	0.847 to 0.922
$LAVi_{preA}$/active LAEF	0.893	0.019	0.856 to 0.930
$LAVi_{preA}$/A	0.888	0.020	0.849 to 0.927
$LAVi_{preA}$/Aa	0.927	0.015	0.897 to 0.956

The sensitivity, specificity, diagnostic accuracy, and positive predictive value for the detection of PAF were determined with an optimal cutoff value according to the ROC analysis, as shown in Table 4. Diagnostic accuracy and positive predictive value of the $LAVi_{preA}$/Aa ratio at the cutoff value of >2.7 mL · m^{-2}/cm · s^{-1} were clearly superior to those of the LAVi of >32.0 mL/m^2.

From the results of univariate analysis for age, sex, body weight, LV hypertrophy, E/Ea, and diabetes mellitus, LV hypertrophy (odds ratio: 2.059 [95% CI: 1.251 to 3.386]; P<0.001) and E/Ea (odds ratio: 1.205 [95% CI: 1.108 to 1.309]; P<0.001) were considered as significant covariates. However, multivariate analysis demonstrated that the $LAVi_{preA}$/Aa ratio was the single significant factor of a history of PAF (odds ratio: 11.786 [95% CI: 6.178 to 22.483]; P<0.001).

LA Size Against Atrial Pump Function

The relationship between LA size and atrial pump function in our population is illustrated in Figure 2. LA size and Aa showed an inverse correlation (LAVi: r=−0.503, P<0.001; $LAVi_{preA}$:

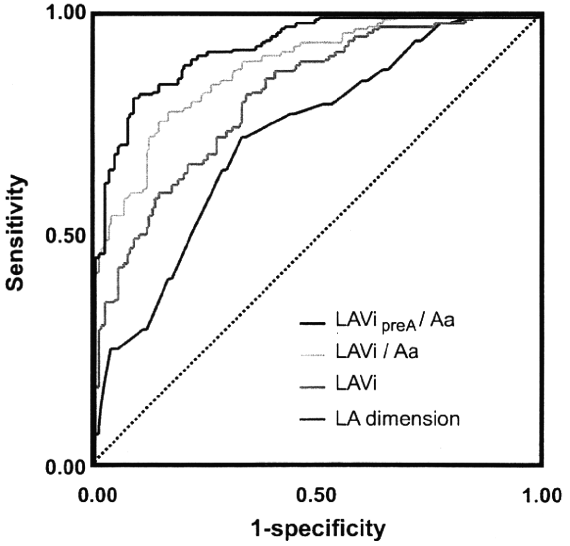

Figure 1. ROC curves for detecting PAF. Comparison of ROC curves for the $LAVi_{preA}$/Aa (red line), LAVi/Aa (yellow line), LAVi (green line), and LA dimension (blue line) values. The AUC values are listed in Table 3.

Table 4. Evaluation of Echocardiographic Parameters According to Sensitivity, Specificity, and Diagnostic Accuracy for Detection of PAF in Hypertensive Patients

Variable	Sensitivity, %	Specificity, %	Diagnostic Accuracy, %	PPV, %
LA dimension >41 mm	72	67	71	69
LAVi >32.0 mL/m^2	82	66	74	71
LAVi/A >0.50 mL · m^{-2}/cm · s^{-1}	75	87	81	85
LAVi/Aa >3.6 mL · m^{-2}/cm · s^{-1}	78	84	82	81
LAVi$_{preA}$/A >0.36 mL · m^{-2}/cm · s^{-1}	80	85	83	84
LAVi$_{preA}$/Aa >2.7 mL · m^{-2}/cm · s^{-1}	82	91	86	90

Values are expressed as percentage. PPV indicates positive predictive value.

$r=-0.458$, $P<0.001$). The PAF group is located disproportionately in the upper left part as compared with the control group. The black dotted lines discriminate best between the PAF and control groups, with slopes of 3.6 (the LAVi/Aa ratio=3.6 mL · m^{-2}/cm · s^{-1}) and 2.7 (the LAVi$_{preA}$/Aa ratio=2.7 mL · m^{-2}/cm · s^{-1}), respectively. The red dotted lines show the lower bound of the PAF group, with slopes of 2.3 and 1.9, respectively.

Discussion

The LA of hypertensive patients with PAF was characterized by further enlargement and impaired pump function as compared with that of hypertensive patients in whom PAF had never been documented. Thus, the ratio of LAVi$_{preA}$ to Aa was most powerful, and the ratio of LAVi to Aa was the next most powerful for differentiating hypertensive patients with a history of PAF.

LA Remodeling in Hypertension

LA size has been reported to serve as a surrogate measure of chronic LV diastolic dysfunction.[27] Hypertension induces an increase in LV wall stress, leading to increased wall thickness, myocyte hypertrophy, and myocardial fibrosis.[28,29] Impaired myocardial relaxation and increased LV diastolic stiffness can cause elevated LV diastolic filling pressure,[30] consistent with the increase in E/Ea. Moreover, long-standing hypertension results in interstitial fibrosis and arrhythmic substrate even in the LA.[31] In a large cohort study, increased LV mass and LA diameter were independently associated with the occurrence of AF in patients with hypertension.[32] Similarly, we found that LV mass index, E/Ea, and LAVi values were significantly increased in our hypertensive patients with PAF compared with those in hypertensive patients without PAF. In addition, LAVi showed a significant correlation with both LV mass index and E/Ea. These findings do not contradict the concept that the occurrence of PAF in hypertension is associated with LA remodeling as a consequence of LA overload because of elevated LV filling pressure.

The LAVi$_{preA}$/Aa and LAVi/Aa ratios showed a very modest but yet significant correlation with the time interval between the first PAF episode and this examination. LA remodeling is thought to progress according to not only the LA overload but also the duration of AF.[33] Thus, the indices that we proposed may be markers representing the degrees of progressive LA remodeling.

Frank-Starling Mechanism of LA Function

According to the Frank-Starling mechanism, contractile force of the ventricular myocardium is proportional to its initial length; this mechanism also applies to the LA myocardium.[22,23] LA pump function is enhanced in response to elevated LV filling pressure as long as the Frank-Starling mechanism holds. Within the range of compensation, therefore, the points in Figure 2 should range toward the upper right direction; in contrast, the points belonging to the PAF group are located in the upper left area. This disproportional distribution is also thought to demonstrate a shift of or a deviation from the Frank-Starling curves because of further progression of atrial remodeling in the PAF group. In addition, Figure 2 shows that patients with an LAVi/Aa ratio ≥2.3 mL · m^{-2}/cm · s^{-1}

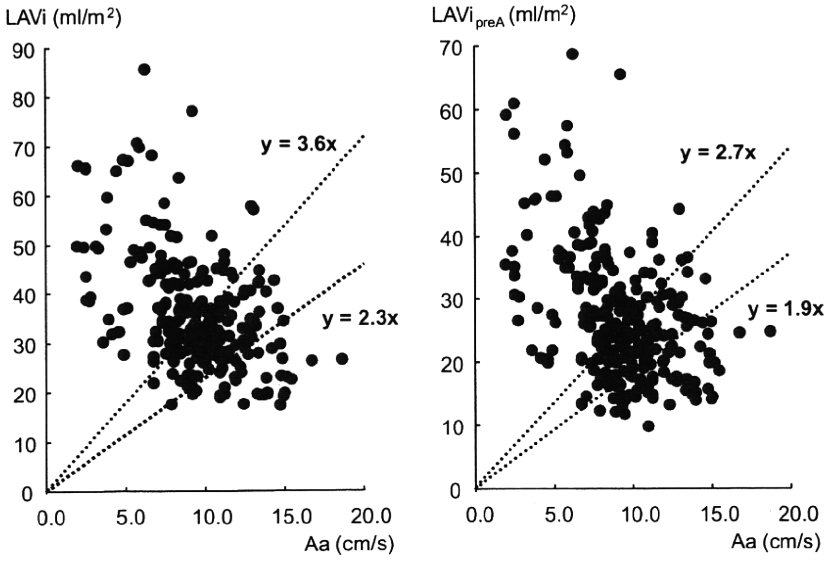

Figure 2. Relationship between LA size and pump function in patients with and without PAF. Scatter diagrams showing the distribution of plots of the LAVi against Aa values (left) and LAVi$_{preA}$ against Aa values (right). Red points indicate hypertensive patients with PAF, and blue points indicate hypertensive patients in whom PAF has never been documented. Patients with LAVi/Aa ratios >2.3 mL · m^{-2}/cm · s^{-1} or LAVi$_{preA}$/Aa ratios >1.9 mL · m^{-2}/cm · s^{-1} may have PAF.

or $LAVi_{preA}$/Aa ratio ≥ 1.9 $mL \cdot m^{-2}/cm \cdot s^{-1}$ may potentially have a history of PAF.

Preload is originally reflected as the initial stretching of cardiac myocytes before contraction. Thus, when adding atrial function to LA size for assessing atrial remodeling, $LAVi_{preA}$ is thought to be physiologically more preferable to LA size than is LAVi. Therefore, it was a reasonable result that the $LAVi_{preA}$/Aa ratio showed better diagnostic ability than the LAVi/Aa ratio.

Measurement of Atrial Pump Function

Several past studies have demonstrated that Aa velocity correlates well with atrial contractile function and can be used as a rapid and accurate marker of atrial function.[16-20] Similar to results of these studies, Aa showed a significant correlation with active LAEF in our study, and the correlation of Aa with active LAEF also remained in patients with excessive LA enlargement.

The changes in flow velocity profile with different positions of the pulsed-wave Doppler sample volume may affect the diagnostic accuracy of the $LAVi_{preA}$/A ratio. Even slight changes in sample volume position can easily cause a decrease in peak A velocity.[34] In contrast, TDI-derived mitral annulus velocities are relatively independent of these problems.[35] Our results also show that Aa is a marker reflecting atrial pump function.

Lateral Aa is a favorable discrimination parameter because its amplitude is greater than that of septal Aa. However, the left lung often attenuates tissue Doppler signals from the lateral annulus margin. The mitral septal annulus motion is always parallel to the Doppler beam, and its measurements are certain. Septal Aa could, however, be influenced by right atrial pump function. In the present study, therefore, we used the average of the septal and lateral Aas.

Study Limitations

First, this was a cross-sectional study. To clarify whether the present index can predict future AF development or complications, further research must provide longitudinal assessments. Second, it is difficult to distinguish whether the impaired atrial pump function was attributed to LA remodeling or showed a recovery process after spontaneous conversion of AF. This issue does not concern the diagnosis of PAF, but it may slightly affect the cutoff value for detecting PAF. Third, atrial reservoir function was not examined in the present study. Some reports indicate that evaluating LA reservoir function using strain or strain rate is useful for the prediction of AF relapse after treatments.[36,37] Nevertheless, we chose to use pulsed TDI parameters for the following reasons: (1) measurement of strain or strain rate with high reproducibility or using the speckle tracking method requires a high-end ultrasound machine and special dedicated software, but pulsed TDI is available on almost all machines; (2) peak late-diastolic atrial strain rate during atrial contraction has been reported to be correlated well with Aa[38,39]; (3) speckle tracking software, which is used when measuring atrial strain or strain rate, is designed primarily for the LV and not the LA; and (4) atrial strain or strain rate reflects only regional function of the LA, and the position of regions of interest for assessing LA global pump function is still controversial, whereas Aa is a marker of atrial global function and has been validated by cardiac catheters.[17] We preferred this general technology because our goal was to make our method accessible. Fourth, we did not measure pulmonary venous flow for assessing LV diastolic function because obtaining an adequate signal for analysis has been reported to be difficult in all subjects.[40,41] Furthermore, a recent consensus statement recommends tissue Doppler velocities as a first-line echocardiographic diagnostic approach to LV diastolic dysfunction.[42] Fifth, obtaining an accurate time interval between the first PAF episode and the current examination was practically difficult because PAF is, by nature, an elusive disease, and the majority of PAF episodes are known to be asymptomatic.[43] Similarly, the first PAF episode in asymptomatic patients was noticed incidentally as an irregularly irregular rhythm during auscultation or palpitating arterial pulse and was confirmed using ECG at a monthly or biweekly consultation day; thus, the interval may be not accurate. Little information on the number and duration of PAF episodes was available in the present study. Finally, we cannot clearly state that self-terminating spontaneous AF was never present in hypertensive patients with PAF within 1 week of examination or in patients with hypertension alone; nonetheless, we addressed this concern by performing repeated 12-lead ECGs, 24-hour Holter monitoring, and strict medical interviews for the subjects of the study.

Perspectives

Our observations that the LA of hypertensive patients with PAF is characterized by dilatation and impaired pump function and that the ratio of LA size to pump function is useful for identifying patients with PAF have important public health and clinical implications. If the presence of PAF is suspected at the time of echocardiography, further examinations and careful monitoring (including repeated 24-hour or event-ECG Holter recording) may be considered. This is especially true for patients with multiple risk factors for stroke (eg, congestive heart failure, hypertension, age >75 years, diabetes mellitus, and previous stroke or transient ischemic attack). In other words, the present indices may be useful for recommending preventive therapy in high-risk patients, because clinicians can prevent the greater part of ischemic stroke from AF with anticoagulation therapy.[44] A recent report from the Framingham Heart Study proposed a risk score for the future development of AF, but echocardiographic parameters provided only slight improvement in the risk assessment score.[45] The measurements derived from the conventional M-mode method may have attenuated the benefits of echocardiography in the aforementioned study. We expect that the new marker presented here (LA size divided by atrial pump function) will improve risk classification in future prospective studies.

Acknowledgments

We thank the members of the Arita Cohort Studies Unit for their valuable assistance with patient investigations, as well as Yoshiyuki Sumita, Tetsuhiro Yamano, Haruhiko Abe, and Takuya Hasegawa for obtaining excellent echocardiographic data.

Sources of Funding

This study was supported by a grant from the Japan Heart Foundation.

Disclosures

None.

References

1. Fleqel KM, Shipley MJ, Rose G. Risk of stroke in non-rheumatic atrial fibrillation. *Lancet.* 1987;1:526–529.
2. Lévy S, Maarek M, Coumel P, Guize L, Lekieffre J, Medvedowsky JL, Sebaoun A. Characterization of different subjects of atrial fibrillation in general practice in France: the ALFA Study. *Circulation.* 1999;99: 3028–3035.
3. Wolf PA, Abbott RD, Kannel WB. Atrial fibrillation as an independent risk factor for stroke: the Framingham Study. *Stroke.* 1991;22:983–988.
4. Connolly SJ, Laupacis A, Gent M, Roberts RS, Cairns JA, Joyner C. Canadian Atrial Fibrillation Anticoagulation (CAFA) Study. *J Am Coll Cardiol.* 1991;18:349–355.
5. Gage BF, Waterman AD, Shannon W, Boechler M, Rich MW, Radford MJ. Validation of clinical classification schemes for predicting stroke: results from the National Registry of Atrial Fibrillation. *JAMA.* 2001; 285:2864–2870.
6. Hohnloser SH, Pajitnev D, Pogue J, Healey JS, Pfeffer MA, Yusuf S, Connolly SJ, for the ACTIVE W Investigators. Incidence of stroke in paroxysmal versus sustained atrial fibrillation in patients taking oral anticoagulation or combined antiplatelet therapy: an ACTIVE W Substudy. *J Am Coll Cardiol.* 2007;50:2156–2161.
7. Fang MC, Go AS, Chang Y, Borowsky L, Pomernacki NK, Singer DE, for the ATRIA Study Group. Comparison of risk stratification schemes to predict thromboembolism in people with nonvalvular atrial fibrillation. *J Am Coll Cardiol.* 2008;51:810–815.
8. Albers GW, Diener HC, Frison L, Grind M, Nevinson M, Partridge S, Halperin JL, Horrow J, Olsson SB, Petersen P, Vahanian A, for the SPORTIF Executive Steering Committee for the SPORTIF V Investigators. Ximelagatran vs warfarin for stroke prevention in patients with nonvalvular atrial fibrillation: a randomized trial. *JAMA.* 2005;293: 690–698.
9. Lewington S, Clarke R, Qizilbash N, Peto R, Collins R, for the Prospective Studies Collaboration. Age-specific relevance of usual blood pressure to vascular mortality: a meta-analysis of individual data for one million adults in 61 prospective studies. *Lancet.* 2002;360:1903–1913.
10. Deroubaix E, Folliguet T, Rücker-Martin C, Dinanian S, Boixel C, Validire P, Daniel P, Capderou A, Hatem SN. Moderate and chronic hemodynamic overload of sheep atria induces reversible cellular electrophysiologic abnormalities and atrial vulnerability. *J Am Coll Cardiol.* 2004;44:1918–1926.
11. Wijffels MC, Kirchhof CJ, Dorland R, Allessie MA. Atrial fibrillation begets atrial fibrillation: a study in awake chronically instrumented goats. *Circulation.* 1995;92:1954–1968.
12. Lang RM, Bierig M, Devereux RB, Flachskampf FA, Foster E, Pellikka PA, Picard MH, Roman MJ, Seward J, Shanewise JS, Solomon SD, Spencer KT, Sutton MS, Stewart WJ, for the Chamber Quantification Writing Group; American Society of Echocardiography's Guidelines and Standards Committee; European Association of Echocardiography. Recommendations for chamber quantification: a report from the American Society of Echocardiography's Guidelines and Standards Committee and the Chamber Quantification Writing Group, developed in conjunction with the European Association of Echocardiography, a branch of the European Society of Cardiology. *J Am Soc Echocardiogr.* 2005;18: 1440–1463.
13. Rodrigues AC, Scannavacca MI, Caldas MA, Hotta VT, Pisani C, Sosa EA, Mathias W Jr. Left atrial function after ablation for paroxysmal atrial fibrillation. *Am J Cardiol.* 2009;103:395–398.
14. Abhayaratna WP, Seward JB, Appleton CP, Douglas PS, Oh JK, Tajik AJ, Tsang TS. Left atrial size: physiologic determinants and clinical applications. *J Am Coll Cardiol.* 2006;47:2357–2363.
15. Manning WJ, Leeman DE, Gotch PJ, Come PC. Pulsed Doppler evaluation of atrial mechanical function after electrical cardioversion of atrial fibrillation. *J Am Coll Cardiol.* 1989;13:617–623.
16. Thomas L, Boyd A, Thomas SP, Schiller NB, Ross DL. Atrial structural remodelling and restoration of atrial contraction after linear ablation for atrial fibrillation. *Eur Heart J.* 2003;24:1942–1951.
17. Nagueh SF, Sun H, Kopelen HA, Middleton KJ, Khoury DS. Hemodynamic determinants of the mitral annulus diastolic velocities by tissue Doppler. *J Am Coll Cardiol.* 2001;37:278–285.
18. Saraiva RM, Yamano T, Matsumura Y, Takasaki K, Toyono M, Agler DA, Greenberg N, Thomas JD, Shiota T. Left atrial function assessed by real-time 3-dimensional echocardiography is related to right ventricular systolic pressure in chronic mitral regurgitation. *Am Heart J.* 2009;158: 309–316.
19. Thomas L, Levett K, Boyd A, Leung DY, Schiller NB, Ross DL. Changes in regional left atrial function with aging: evaluation by Doppler tissue imaging. *Eur J Echocardiogr.* 2003;4:92–100.
20. Khankirawatana B, Khankirawatana S, Peterson B, Mahrous H, Porter TR. Peak atrial systolic mitral annular velocity by Doppler tissue reliably predicts left atrial systolic function. *J Am Soc Echocardiogr.* 2004;17: 353–360.
21. Barbier P, Alioto G, Guazzi MD. Left atrial function and ventricular filling in hypertensive patients with paroxysmal atrial fibrillation. *J Am Coll Cardiol.* 1994;24:165–170.
22. Anwar AM, Geleijnse ML, Soliman OI, Nemes A, ten Cate FJ. Left atrial Frank-Starling law assessed by real-time, three-dimensional echocardiographic left atrial volume changes. *Heart.* 2007;93:1393–1397.
23. Stefanadis C, Dernellis J, Toutouzas P. A clinical appraisal of left atrial function. *Eur Heart J.* 2001;22:22–36.
24. Pickering TG, Hall JE, Appel LJ, Falkner BE, Graves J, Hill MN, Jones DW, Kurtz T, Sheps SG, Roccella EJ, for the Subcommittee of Professional and Public Education of the American Heart Association Council on High Blood Pressure Research. Recommendations for blood pressure measurement in humans and experimental animals: part 1–blood pressure measurement in humans: a statement for professionals from the Subcommittee of Professional and Public Education of the American Heart Association Council on High Blood Pressure Research. *Hypertension.* 2005;45:142–161.
25. Devereux RB, Dahlof B, Levy D, Pfeffer MA. Comparison of enalapril versus nifedipine to decrease left ventricular hypertrophy in systemic hypertension (the PRESERVE Trial). *Am J Cardiol.* 1996;78:61–65.
26. Dokainish H, Zoghbi WA, Lakkis NM, Al-Bakshy F, Dhir M, Quinones MA, Nagueh SF. Optimal noninvasive assessment of left ventricular filling pressures: a comparison of tissue Doppler echocardiography and B-type natriuretic peptide in patients with pulmonary artery catheters. *Circulation.* 2004;109:2432–2439.
27. Pritchett AM, Mahoney DW, Jacobsen SJ, Rodeheffer RJ, Karon BL, Redfield MM. Diastolic dysfunction and left atrial volume: a population-based study. *J Am Coll Cardiol.* 2005;45:87–92.
28. Weber KT, Brilla CG, Janicki JS. Myocardial fibrosis: functional significance and regulatory factors. *Cardiovasc Res.* 1993;27:341–348.
29. Kai H, Kuwahara F, Tokuda K, Imaizumi T. Diastolic dysfunction in hypertensive hearts: roles of perivascular inflammation and reactive myocardial fibrosis. *Hypertens Res.* 2005;28:483–490.
30. Leite-Moreira AF, Correia-Pinto J, Gillebert TC. Afterload induced changes in myocardial relaxation: a mechanism for diastolic dysfunction. *Cardiovasc Res.* 1999;43:344–353.
31. Choisy SC, Arberry LA, Hancox JC, James AF. Increased susceptibility to atrial tachyarrhythmia in spontaneously hypertensive rat hearts. *Hypertension.* 2007;49:498–505.
32. Verdecchia P, Reboldi G, Gattobigio R, Bentivoglio M, Borgioni C, Angeli F, Carluccio E, Sardone MG, Porcellati C. Atrial fibrillation in hypertension: predictors and outcome. *Hypertension.* 2003;41:218–223.
33. Petersen P, Kastrup J, Brinch K, Godtfredsen J, Boysen G. Relation between left atrial dimension and duration of atrial fibrillation. *Am J Cardiol.* 1987;60:382–384.
34. Appleton CP, Jensen JL, Hatle LK, Oh JK. Doppler evaluation of left and right ventricular diastolic function: a technical guide for obtaining optimal flow velocity recordings. *J Am Soc Echocardiogr.* 1997;10: 271–292.
35. De Boeck BW, Cramer MJ, Oh JK, van der Aa RP, Jaarsma W. Spectral pulsed tissue Doppler imaging in diastole: a tool to increase our insight in and assessment of diastolic relaxation of the left ventricle. *Am Heart J.* 2003;146:411–419.
36. Di Salvo G, Caso P, Lo Piccolo R, Fusco A, Martiniello AR, Russo MG, D'Onofrio A, Severino S, Calabró P, Pacileo G, Mininni N, Calabró R. Atrial myocardial deformation properties predict maintenance of sinus rhythm after external cardioversion of recent-onset lone atrial fibrillation: a color Doppler myocardial imaging and transthoracic and transesophageal echocardiographic study. *Circulation.* 2005;112:387–395.

37. Schneider C, Malisius R, Krause K, Lampe F, Bahlmann E, Boczor S, Antz M, Ernst S, Kuck KH. Strain rate imaging for functional quantification of the left atrium: atrial deformation predicts the maintenance of sinus rhythm after catheter ablation of atrial fibrillation. *Eur Heart J.* 2008;29:1397–1409.
38. Eshoo S, Boyd AC, Ross DL, Marwick TH, Thomas L. Strain rate evaluation of phasic atrial function in hypertension. *Heart.* 2009;95:1184–1191.
39. Thomas L, McKay T, Byth K, Marwick TH. Abnormalities of left atrial function after cardioversion: an atrial strain rate study. *Heart.* 2007;93:89–95.
40. Kasner M, Westermann D, Steendijk P, Gaub R, Wilkenshoff U, Weitmann K, Hoffmann W, Poller W, Schultheiss HP, Pauschinger M, Tschöpe C. Utility of Doppler echocardiography and tissue Doppler imaging in the estimation of diastolic function in heart failure with normal ejection fraction: a comparative Doppler-conductance catheterization study. *Circulation.* 2007;116:637–647.
41. Quiñones MA, Otto CM, Stoddard M, Waggoner A, Zoghbi WA, for the Doppler Quantification Task Force of the Nomenclature and Standards Committee of the American Society of Echocardiography. Recommendations for quantification of Doppler echocardiography: a report from the Doppler Quantification Task Force of the Nomenclature and Standards Committee of the American Society of Echocardiography. *J Am Soc Echocardiogr.* 2002;15:167–184.
42. Paulus WJ, Tschöpe C, Sanderson JE, Rusconi C, Flachskampf FA, Rademakers FE, Marino P, Smiseth OA, De Keulenaer G, Leite-Moreira AF, Borbély A, Edes I, Handoko ML, Heymans S, Pezzali N, Pieske B, Dickstein K, Fraser AG, Brutsaert DL. How to diagnose diastolic heart failure: a consensus statement on the diagnosis of heart failure with normal left ventricular ejection fraction by the Heart Failure and Echocardiography Associations of the European Society of Cardiology. *Eur Heart J.* 2007;28:2539–2350.
43. Rho RW, Page RL. Asymptomatic atrial fibrillation. *Prog Cardiovasc Dis.* 2005;48:79–87.
44. Hart RG, Pearce LA, Aguilar MI. Meta-analysis: antithrombotic therapy to prevent stroke in patients who have nonvalvular atrial fibrillation. *Ann Intern Med.* 2007;146:857–867.
45. Schnabel RB, Sullivan LM, Levy D, Pencina MJ, Massaro JM, D'Agostino RB Sr, Newton-Cheh C, Yamamoto JF, Magnani JW, Tadros TM, Kannel WB, Wang TJ, Ellinor PT, Wolf PA, Vasan RS, Benjamin EJ. Development of a risk score for atrial fibrillation (Framingham Heart Study): a community-based cohort study. *Lancet.* 2009;373:739–745.

nature
cell biology

AMPK controls the speed of microtubule polymerization and directional cell migration through CLIP-170 phosphorylation

Atsushi Nakano[1,4], Hisakazu Kato[3,4], Takashi Watanabe[5,6], Kyung-Duk Min[1,3], Satoru Yamazaki[1], Yoshihiro Asano[3,4], Osamu Seguchi[1], Shuichiro Higo[3], Yasunori Shintani[3], Hiroshi Asanuma[1], Masanori Asakura[1], Tetsuo Minamino[3], Kozo Kaibuchi[6], Naoki Mochizuki[2], Masafumi Kitakaze[1] and Seiji Takashima[3,4,7]

AMP-activated protein kinase (AMPK) is an energy-sensing Ser/Thr protein kinase originally shown to be regulated by AMP[1]. AMPK is activated by various cellular stresses that inhibit ATP production or stimulate ATP consumption[2]. In addition to its role in metabolism, AMPK has recently been reported to reshape cells by regulating cell polarity and division[3–6]. However, the downstream targets of AMPK that participate in these functions have not been fully identified. Here, we show that phosphorylation of the microtubule plus end protein CLIP-170 by AMPK is required for microtubule dynamics and the regulation of directional cell migration. Both inhibition of AMPK and expression of a non-phosphorylatable CLIP-170 mutant resulted in prolonged and enhanced accumulation of CLIP-170 at microtubule tips, and slower tubulin polymerization. Furthermore, inhibition of AMPK impaired microtubule stabilization and perturbed directional cell migration. All of these phenotypes were rescued by expression of a phosphomimetic CLIP-170 mutant. Our results demonstrate, therefore, that AMPK controls basic cellular functions by regulating microtubule dynamics through CLIP-170 phosphorylation.

Besides the metabolic activity of AMPK, there is growing evidence that AMPK and its upstream kinase liver kinase B1 (LKB1) have pivotal roles in the establishment of cell polarity and cell division[7,8] in *Drosophila melanogaster*[6,9] and *Caenorhabditis elegans*[10]. In mammalian cells, AMPK is associated with tight junction assembly, and regulates epithelial polarity[3,4].

To discover previously unidentified substrates of AMPK, we performed a unique screen using two-step column chromatography combined with an *in vitro* kinase reaction. Using mouse heart homogenates, we purified and identified a cytoplasmic linker protein CLIP-170, which has a relative molecular mass of 170,000 (M_r 170K) and is a substrate of AMPK (Supplementary Information, Fig. S1). CLIP-170 is one of the microtubule plus end proteins originally identified as proteins that bind endocytic vesicles to microtubules[11,12]. CLIP-170 directly binds freshly polymerized distal ends of growing microtubules and rapidly dissociates from the older microtubule lattice[13]. However, a direct link between CLIP-170 and physiological control of cell function has not been fully elucidated. Both recombinant AMPK made by 293T cells and AMPK purified from rat liver efficiently phosphorylated recombinant CLIP-170 (Fig. 1a). Phospho amino acid analysis revealed that AMPK phosphorylates a Ser residue of CLIP-170 (Fig. 1b). A combination of mass spectrometric and multiple mutation analyses of CLIP-170 identified Ser 311 as the only AMPK phosphorylation site. AMPK did not phosphorylate CLIP-115, a close mammalian homologue of CLIP-170, or Ser 737 of CLIP-170, demonstrating an AMPK substrate consensus sequence[14] (Fig. 1c). Recombinant glutathione S-transferase (GST)-fused wild-type CLIP-170 and a Ser 311-to-Ala mutant (S311A) of CLIP-170 were produced in *Escherichia coli*. The wild-type, but not the S311A mutant, was phosphorylated by AMPK and 0.29 mole of phosphate per mole of CLIP-170 was incorporated, indicating that Ser 311 of CLIP-170 is phosphorylated directly by AMPK (Fig. 1d). Next, we generated an antibody against Ser 311-phosphorylated CLIP-170 (p-CLIP-170). The specificity and sensitivity of this antibody were confirmed by the following observations: first the p-CLIP-170 antibody exclusively detected p170 as a single band, even when total cell lysates were assessed; and second, it did not recognize phosphatase-treated p170 (Fig. 1e). Analyses using this antibody also demonstrated the specific phosphorylation of CLIP-170 at Ser 311 by AMPK (Fig. 1f). The amino acid sequence surrounding Ser 311 matches the consensus sequence of a potential AMPK phosphorylation site and is well conserved among various species (Fig. 1g).

[1]Division of Cardiovascular Medicine, National Cardiovascular Center and [2]Department of Structural Analysis, National Cardiovascular Center, Research Institute Suita, Osaka 565-8565, Japan. [3]Department of Cardiovascular Medicine and [4]Department of Molecular Cardiology, Osaka University Graduate School of Medicine Suita, Osaka 565-0871, Japan. [5]Institute for Advanced Research, Nagoya University Graduate School of Medicine and [6]Department of Cell Pharmacology, Nagoya University Graduate School of Medicine, Nagoya, Aichi 466-8550, Japan.
[7]Correspondence should be addressed to S.T. (e-mail: takasima@medone.med.osaka-u.ac.jp)

Received 4 March 2010; accepted 29 April 2010; published online 23 May 2010; DOI: 10.1038/ncb2060

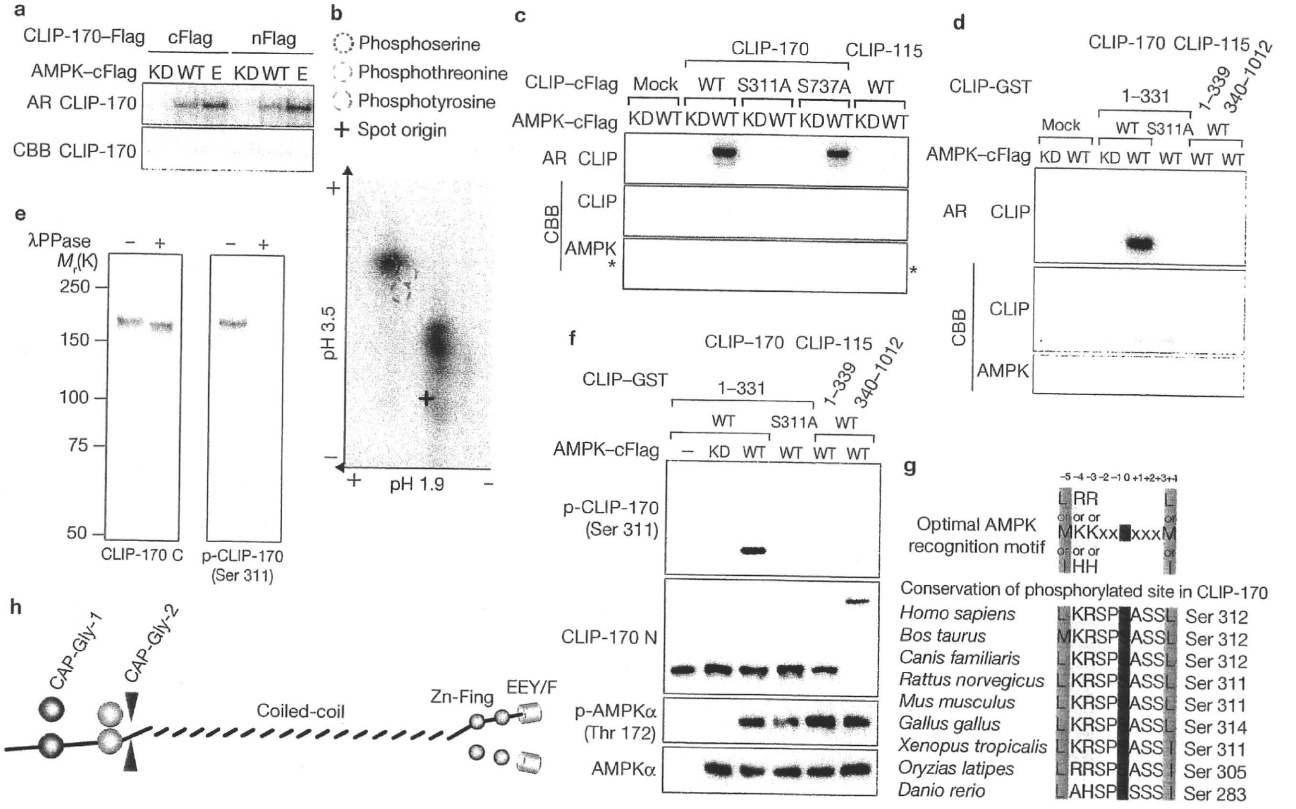

Figure 1 *In vitro* phosphorylation of CLIP-170 Ser311 by AMPK. (**a**) An autoradiographic (AR) image of mammalian recombinant carboxy-terminally (cFlag) or amino-terminally (nFlag) Flag-tagged CLIP-170 incubated with either recombinant kinase dead (KD), wild-type (WT) or endogenous (E) AMPK. (**b**) Phospho-amino acid analysis of CLIP-170 phosphorylated by AMPK. Only a Ser residue was phosphorylated (radioactivity indicated by the red circle). (**c**) An AR of mammalian recombinant cFlag-tagged CLIP-170 (WT, S311A and S737A) and CLIP-115 (WT) incubated with recombinant KD or WT AMPK. AMPK is indicated by an asterisk. (**d**) An AR image of GST fusion proteins representing amino acids 1–331 of CLIP-170 (WT or S311A), or either the N (1–339) or the C (340–1012) terminus of CLIP-115 incubated with KD or WT AMPK. (**e**) Lysate of Vero cells treated with or without phosphatase (λPPase) was subjected to immunoblot analysis with an antibody against the C terminus of CLIP-170 (CLIP-170 C) and a Ser 311 phosphospecific antibody (p-CLIP-170). (**f**) Immunoblot analysis of the GST-fused CLIP constructs described above with KD or WT AMPK. These samples were blotted using a p-CLIP-170 and a non-phosphospecific antibody against the N terminus of CLIP-170 (CLIP-170 N). CLIP-170 N also recognized CLIP-115. (**g**) The optimal AMPK recognition motif. The consensus sequence of AMPK is identical to the sequence around Ser 311 of CLIP-170. This residue is highly conserved among various species. (**h**) Structural model of CLIP-170. Ser 311 is located between the CAP-Gly-2 domain and the coiled-coil region in CLIP-170. Ser 311 is indicated by red arrowheads. CAP-Gly, cytoskeleton-associated protein Gly-rich; Zn-Fing, C-terminal zinc knuckle of CLIP-170; EEY/F, C-terminal amino sequence of CLIP-170; CBB, Coomassie brilliant blue staining. Uncropped images of blots are shown in Supplementary Information, Fig. S5.

Ser 311 is located between a Gly-rich microtubule-binding domain (cytoskeleton-associated protein Gly-rich; CAP-Gly) and a coiled-coil domain (Fig. 1h).

Next, we examined AMPK-induced CLIP-170 phosphorylation in cultured cells. Compound C, an inhibitor of AMPK, reduced the phosphorylation level of CLIP-170 (Fig. 2a), whereas the AMPK activator AICAR (5-aminoimidazole-4-carboxyamide ribonucleoside) did not affect CLIP-170 phosphorylation (Supplementary Information, Fig. S2a). The phosphorylation level of acetyl-CoA carboxylase (ACC), which was used as a control, reflected the conventional responses of cells to both Compound C and AICAR. Although Compound C is an inhibitor of AMPK, it can also inhibit several other kinases[15]. Therefore, we used short interfering RNAs (siRNAs) to specifically deplete AMPK. Depletion of AMPK with siRNAs specific for either the α_1 or the α_2 catalytic subunit also reduced CLIP-170 phosphorylation (Fig. 2b). These data indicate that phosphorylation of CLIP-170 at Ser 311 is regulated endogenously by AMPK. To explore the significance of AMPK-induced CLIP-170 phosphorylation, we first immunocytochemically investigated the localization of phosphorylated CLIP-170 in cultured cells. A non-phospho-specific antibody (CLIP-170 C), as well as a Ser 311 phospho-specific antibody (p-CLIP-170), stained the plus ends of microtubules (Fig. 2c, d). To distinguish between the total CLIP-170 population and phosphorylated CLIP-170, Vero cells stably expressing CLIP-170–EGFP were stained with these antibodies. The pattern observed with the CLIP-170 C antibody (red or yellow) completely matched that of CLIP-170–EGFP (Fig. 2e, green), suggesting that CLIP-170–EGFP mimics the localization of endogenous CLIP-170. By contrast, p-CLIP-170 staining mostly overlapped with CLIP-170–EGFP but was located predominantly on the distal side (red or yellow) of CLIP-170–EGFP (Fig. 2f, green). This result suggests that phosphorylated CLIP-170 attaches to microtubules at the more distal end, compared with non-phosphorylated CLIP-170. A marked change in CLIP-170 localization was observed when these cells were treated with Compound C: CLIP-170–EGFP accumulated significantly farther along the length of the microtubules (Fig. 2g, h, green). CLIP-170 C staining again overlapped with CLIP-170–EGFP (Fig. 2g, red or yellow), whereas p-CLIP-170 staining was markedly reduced and localized as only a tiny